Int. J. Electrochem. Sci., 12 **(2017)** 4301 – 4318, doi: 10.20964/2017.05.67

International Journal of ELECTROCHEMICAL SCIENCE
www.electrochemsci.org

Novel Aminated Cellulose Acetate Membranes for Direct Methanol Fuel Cells (DMFCs)

M. S. Mohy Eldin[1,2,*], *A. M. Omer*[2*], *T. M. Tamer*[2], *M. H. Abd Elmageed* [3], *M. E. Youssef*[4], *R. E. Khalifa*[2]

[1] Chemistry Department, Faculty of Science, University of Jeddah, Asfan, P. O. Box: 80203, Jeddah 21589, Saudi Arabia
[2] Polymer Materials Research Department, Advanced Technology and New Materials Research Institute, SRTA-City, New Borg El-Arab City 21934, Alexandria, Egypt
[3] Chemical Engineering Department, Faculty of Engineering, Alexandria University, Alexandria, Egypt.
[4] Computer-Based Engineering Applications Department, Informatics Research Institute, MUCSAT, New Borg El-Arab City 21934, Alexandria, Egypt
[*]E-mail: m.mohyeldin@mucsat.sci.eg, Ahmedomer_81@yahoo.com

Received: 8 July 2016 / *Accepted:* 19 January 2017 / *Published:* 12 April 2017

Currently, enhancing the mechanical properties and decreasing methanol permeability is the major challenge for the polyelectrolyte membranes for the direct methanol fuel cells (DMFCs). In this study, novel aminated proton exchange membrane based on cellulose acetate (CA) for DMFC were prepared via activation process using epichlorohydrin (ECH) afterward amination reaction using ethylene di-amine (EDA). The structure of the aminated cellulose acetate membranes (AMCA) were investigated by a Fourier transform infrared spectroscopy, Scanning electron microscopy, Thermogravimetric analysis. The adsorption of the AMCA membrane of water and methanol solution was also characterized. Additionally, the AMCA membranes were investigated as a function of a molar ratio of EDA concerning ion exchange capacity (IEC), dimensional stability, thickness change, thermal oxidation stability, and methanol permeability in detail. Results revealed that the modified CA membranes have excellent dimensional stability, admirable physicomechanical properties (32.13 N) and low methanol permeability (4.54*10-17 cm2/S) compared to 1.14*10-9 cm2/S for commercial Nafion®117 membranes. Furthermore, the membrane performance with various contents of EDA showed a vast improvement compared to Nafion®117. In conclusion, the obtained series of AMCA membranes offering the possibilities to reduce the DMFC membrane cost considerably while keeping high performance. These results suggested that these membranes are quite attractive candidates as an innovative polymeric electrolyte material for DMFCs applications.

Keywords: Proton exchange membranes; Cellulose acetate; Methanol permeability; Ethylene di-amine; Direct methanol fuel cell.

1. INTRODUCTION

Electricity is the highest rising type of power. Though it is being used more professionally, and regardless the development to use fuels other than oil, the industrial electricity field still faces some significant challenges, one of the most critical of which is community anxiety about the environmental issues as a result of electricity production and use [1]. The other is road transport sector as it required a notable diversification of energy resources with minimum associated harmful emissions. In the last few decades, the consequential bend of socio-economic policies towards greener alternatives has led to extensive research into the development of fuel cell (FC) technology [2]. Fuel cells FCs are alternative electrochemical devices that utilize selective hydrogen based chemicals as fuel to convert chemical energy directly into electrical power, water, and heat on condition that both fuel and oxidant fed continuously to electrodes (anode and cathode compartments). Also, FCs will enable to limit the stress for fossil fuel and additional nuclear-derived energy.

Nowadays, there are many types of developed FCs. Notably, proton exchange membrane fuel cells (PEMFCs) that use a polymer electrolyte membrane (PEM). Defiantly, DMFCs are quite similar to PEMFCs in their structure and working principles [3]. Besides, PEM is considered one of the vital workings parts in DMFC's systems because it acts as a barrier to fuels cross leads between electrolyte as well as for transporting protons from anode to cathode [4-5]. Recently, DMFC is attracted considerable attention as a potential FC system mainly for portable devices as cell phones and laptops and vehicles such as cars, buses, and trucks [6]. Owing to their advantages on employing easily storage and transported liquid fuel (methanol), low operating temperatures, short starting times, noiseless, scalability, low emissions, simple design, energy conversion efficiency, high power density, environmental issues [7-8]. However, the performance and effectiveness of DMFCs are limited by catalyst poisoning caused by CO, an elevated flux of fuel through the PEM, in addition to the resulted resistance among electrodes and PEM [9]. For the PEMs, high ionic conductivity (IC), outstanding mechanical characteristics, chemical stability, are the essential requirements. Moreover, low methanol crossover and swelling ratio of PEM are needed to satisfy applications in DMFCs [10-12]. Currently, Nafion manufactured by DuPont are the primarily PEM used in DMFC. Nafion is suitable for PEMFCs running below 80 oC due to their high IC especially in the hydrated condition [13], reasonable mechanical strength, and excellent electrochemical stability [14-15]. However, Nafion membranes suffer from some drawbacks which limit their efficacy and performance, for instance; high production expenditure, high methanol crossover, and little proton conductivity (PC) either at the higher temperature or lower humidity [16–17]. Therefore, the development of other unconventional membrane resources that can conquer these shortcomings is of importance and necessity [18].

Recently, two classes of alternative PEM materials have been explored for DMFC applications [19]. The first is a low expensive block copolymer with varied electro- mechanical characteristics, adequate stability, and high efficiency. For example polyethyleneimine (PEI) [20], polysulfone Udel® [21] (PSU), sulfonated poly ether- ether ketone (SPEEK) [22], sulfonated polyimide (SPI) [23], sulfonated (styrene ethylene butylenes styrene) (SEBS) [24], sulfonated polybenzimidazole (PBl) [25-27], polyphosphazene [28], and poly(phthalazinone) [29], poly phthalazinone ether ketone [30], poly (2,6-dimethyl-1,4-phenylene oxide) [31], sulfonated poly arylene ether ketone [32], poly phenyl

sulfide sulfone [33]. The further is organic-inorganic composites [34] with a nano size interface amid organic and inorganic domains, which allow outstanding opportunities to generate supplies with exceptional properties. All of these membranes can advance methanol permeability greatly. Also, numerous families of natural and synthetic polymers with various chemical formulas and different strategies for the integration of functional groups have been investigated. such as chitosan (CS) [35], alginate [36], poly vinyl alcohol (PVA) [37], poly vinyl chloride (PVC), poly vinylidene di fluoride (PVDF), fluorinated ethylene propylene (FEP) lately as PEM materials. In our preliminary work innovative CA polymeric structure with sulfonic and phosphonic chains have been fabricated for the first time as PEMs for DMFCs [38, 39]. These membranes showed enhanced thermal and mechanical stability and high methanol resistance than Nafion.

In the current study, an innovative succession of CA with aminated side chain was synthesized via direct reaction with EDA. AMCA membranes were readily synthesized using solution casting technique. Numerous factors affecting modification process were studied to establish the optimum conditions. The prepared membranes were characterized using FTIR spectroscopy to verify chemical structures and thermal stabilities were investigated by TGA. Furthermore, thermal oxidative stability, dimensional change, water and methanol uptakes, and mechanical properties of the prepared films were also considered. More importantly, a DMFC performance was finally observed.

2. EXPERIMENTAL

2.1. Materials

CA powder (40% acetylation degree) and ECH (99.5% purity) provided by Sigma Aldrich Chemie Gmbh (USA). Methanol (99.8% purity) and Sulfuric acid (95-97% purity) provided from Fluka Chemie GmbH (Switzerland). Ethanol absolute, hydrogen Peroxide Sodium Hydroxide and Phenol phethalin obtained from El Nasr Pharmaceutical Company for Chemicals (Egypt). Hydrochloric acid (37% purity) purchased from Polskia Odczynniki Chimiczne S.A. (Finland).

2.2. Methods

2.2.1. Membrane preparation

Amination step

Briefly, CA was firstly activated using ECH as discussed in our preceding work [38]. Then, the activated cellulose acetate (ACA) solution was reacted with different molar ratios of EDA (0.25- 1 M); Scheme 1. The reaction carried out at various time intervals (2–10 h) in a water bath at different temperatures (25–65 °C). After that, the modified CA solution was cast and dried at 45 °C. Finally, the aminated cellulose acetate (AMCA) films were washed with distilled water to eliminate the unreacted EDA.

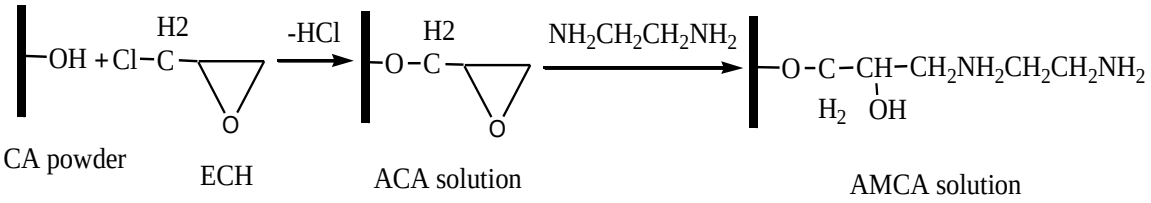

Scheme 1: Reaction mechanism of AMCA.

2.2.2. Membrane characterization

Water and methanol uptakes (LU)

All prepared samples (2 cm × 2 cm) were dehydrated in a vacuum oven for at least 12 hr at 40 ^{o}C and then weighed in the dry state. Followed by immersing in a closed glass container containing water or methanol at room temperature overnight. Later, the distended AMCA membranes were separated, and their surface was wiped gently with filter paper. LU was represented by the variation in weights before and after soaking, and results are the average of three samples [40]:

$$LU(\%) = \frac{W_w - W_d}{W_d} \times 100 \quad (1)$$

Where: W_d and W_w are the dry and the wet weight of the AMCA membranes, respectively.

Dimensional change (ΔA %)

The changes in membrane area (ΔA %) after soaking in water or methanol for 24 h at ambient temperature was calculated as follows [41]:

$$\Delta A\% = \frac{A - A_o}{A_o} \times 100 \quad (2)$$

Where: A_0 and A is the worked area before and after immersing step, respectively.

FTIR

Analysis of the chemical structure of original, ACA, and AMCA films was conducted using FTIR spectroscopy (Shimadzu FTIR-8400 S), made in Japan.

TGA

Thermal stability of CA, ACA, and AMCA membranes was tested using thermal gravimetrical analysis in N_2 atmosphere under 20 °C/min heating rate (Shimadzu TGA-50), made in Japan.

SEM

Scanning of all membrane surfaces was conducting via X- ray energy dispersive device (Joel 6360LA), made in Japan.

Surface roughness

The change in membrane roughness (4cm×5cm) was determined by surface roughness apparatus (SJ- 201P, Japan). The obtained results are mainly the average of at least six measurements.

Thermal oxidation stability

Thermal oxidation stability was conducted by immersing membrane samples (2cm×2cm) in Fenton's reagent (4ppm of ferrous sulfate ($FeSO_4$) in 3% hydrogen peroxide (H_2O_2)). Membrane strips kept under stirring at 80°C and detached from Fenton's solution at regular intervals then dried by tissue paper and weighed quickly [38].

Optical properties (Colorimeter)

The change in color after modification step was considered at different sites via a colorimeter (X-Rite, Sp64 USA) [38]. The color parameters were calculated by:

$$\Delta E = \sqrt{\left(\Delta L^*\right)^2 + \left(\Delta a^*\right)^2 + \left(\Delta b^*\right)^2} \quad (3)$$

Where: ΔL^*, Δa^*, and Δb^* are the standard color factors whereas, L*, a*, and b* are the color stricture of the tested samples.

2.2.3. Ion exchange capacity (IEC)

An identified weight of AMCA membrane was placed in a particular volume of 0.1 M H2SO4 solution, and the mixture was stirred and set aside for at least 12 h. Then; the mixture is filtered, and titrated against NaOH solution. Similarly, control titration in the absence of membranes was also done. At last, IEC was designed by the following equation:

$$IEC = \frac{\left(V_2 - V_1\right)N}{w} \quad (4)$$

Where: V_1 and V_2 are NaOH volumes required for neutralization completion in the absence and the presence of the membrane. N is NaOH normality and w is the sample weight.

Methanol permeability measurements

Methanol crossover across PEM was measured suing a two compartments glass diffusion cell

[42] having an identical volume of 100 ml and one side (A) containing aqueous methanol solution (2M), and the other part (B) includes distilled water (Figure 1). The membrane was firstly hydrated by soaking at least 24 hr in distilled water. Then the film samples were fixed between the two sides under permanent stirring. A micro-syringe was used to withdrawn 500 µL of sample solution every 25 min for 2 h at 25 ^{o}C. Subsequently, methanol concentration was determined using HPLC, and it is correlated to time via the following formula [43]:

$$C_B(t) = \frac{A \times P}{V_B \times L} C_A(t - t_o) \quad (5)$$

Where: P is the methanol permeability coefficient; C_B is methanol concentration in water partition (B) at certain time t. CA is the preliminary methanol concentration in section (A). While A is the film area, L is the film thickness; V_B is the capacity of water partition, and finally t is the time interval. Theoretically, P can be calculated from the relationship between C_B and t as follows [44]:

$$P = \alpha \frac{V_B}{A} \times \frac{L}{C_A} \quad (6)$$

Where: α is referred as the linear line slope between CB against t.

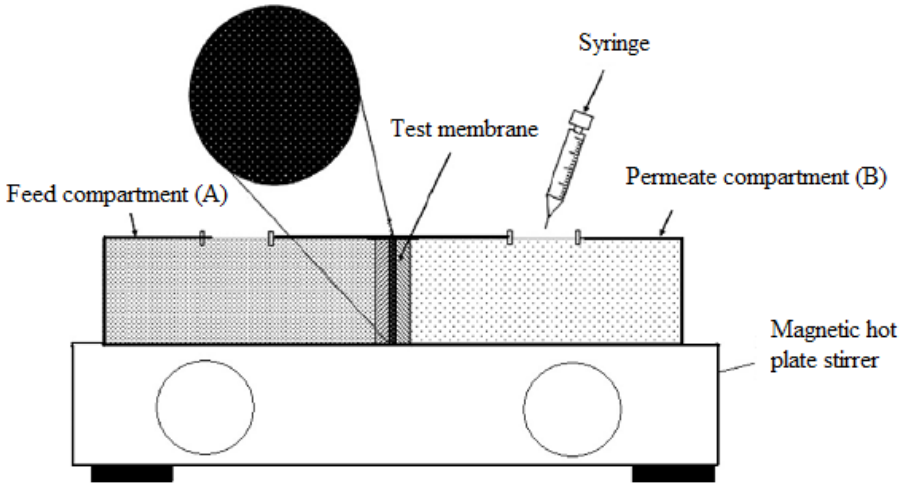

Figure 1: The Simple design of a homemade glass diffusion cell.

Tensile strength test (TS)

LLOYD Instrument 10K was used for tensile strength measurements which considered as a direct indication of the impact of straight tension on membranes behavior. Also, TS is known as the required energy for broking a sample strip, with a specified dimension. The reported results were the average of three measurements [38].

3. RESULTS AND DISCUSSION

3.1. Amination step

3.1.1. Effect of EDA concentration

The consequence of EDA variation in molar ratios on the IEC of AMCA membranes was illustrated in Figure 2. It was indicated that IEC was increased linearly with the rise in EDA concentration from 0.25 to 1M. However, additional raise of EDA levels has no noteworthy effect. This manner may be due to the increase of the primary amine group's number attached to the epoxy groups [45].

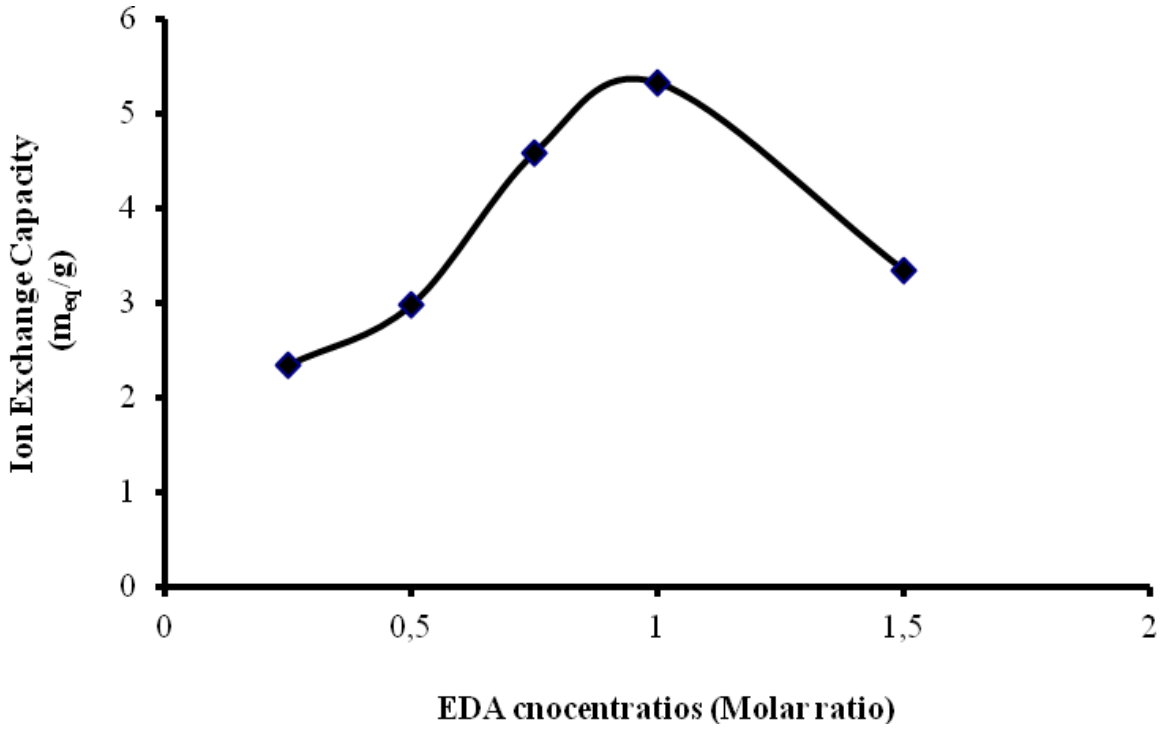

Figure 2. Effect of EDA concentration on the IEC of AMCA membranes at 45 °C for 8 h.

3.1.2. Effect of amination temperature

Figure 3 demonstrates the outcome of temperature variation of EDA on the IEC of AMCA membranes. It was evident that the IEC is considerably affected by the increase in temperature from 25 to 45 °C. The elevating temperature typically causes a direct increase in the reaction rate owing to the diffusion of EDA into the interior polymer matrix, which accordingly improves the membranes hydrophilicity. Prolonged reaction time (8 h), plus homogeneous reaction medium also help in accelerating the reaction and thus decrease the effect of raising reaction temperature above 45 ^{o}C.

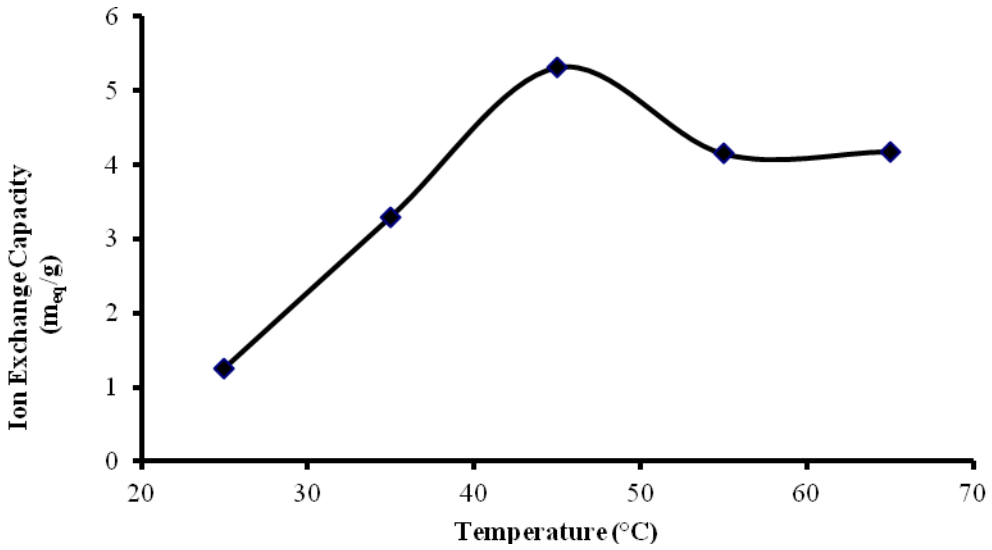

Figure 3. Effect of amination temperature on the IEC of AMCA membranes using 1M EDA for 8 h.

3.1.3. Effect of amination time

The consequence of amination time variation of EDA on the IEC of AMCA membranes was revealed in Figure 4. It was cleared that the IEC are related to the reaction time as it increases with raising the reaction time to achieve a maximum value at 8 h. In contrast, more increase in the amination time up to 10 h has a negligible effect. This action may be interpreted on the proposed reaction between imides group and active sites.

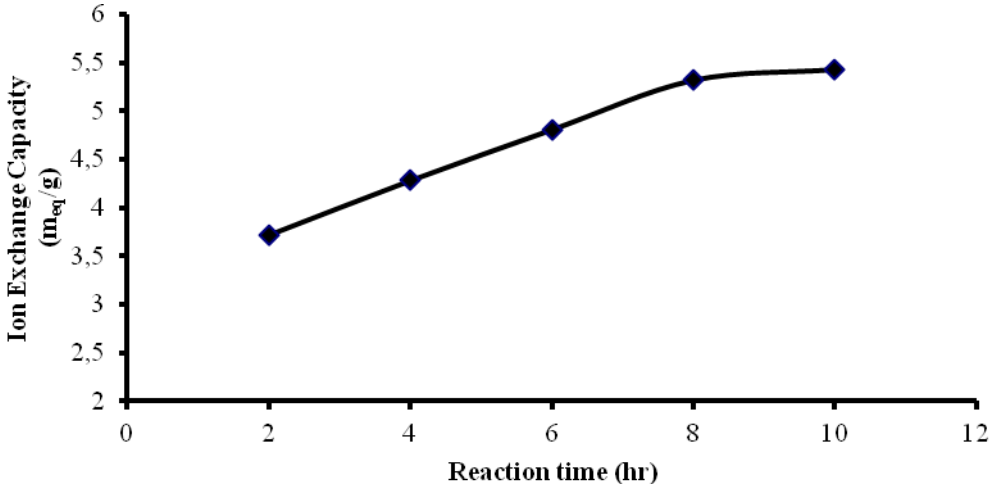

Figure 4. Effect of amination time on the IEC of AMCA membranes using 1M EDA at 45 °C.

3.2. Membranes characterization

3.2.1. Water and methanol uptakes (LU)

It is well known that water content in PEMs is a very critical feature for proton transfer. It was

comprehensible from results that the water and methanol uptake for all AMCA membranes are more than that of CA and ACA membranes. These findings can be attributed to the rise of the hydrophilicity of AMCA membranes. Water and methanol uptake of AMCA membranes at different EDA concentrations and amination time are illustrated in Figures 5 (a and b). It was apparent from Figure 6 that the water uptake and IEC had the same trend as they increase with growing the EDA concentrations from 0.25 to 2 M. With increasing EDA concentration, the polymer hydrophilicity is improved, resulting in high absorption of water, ultimately facilitating enhanced proton transfer. Highly water uptake is an indication for the presence of ion rich zones where proton migration involves ions as H_3O^+ and H_2O5^+ desirable for high proton conduction is enhanced [38, 46].

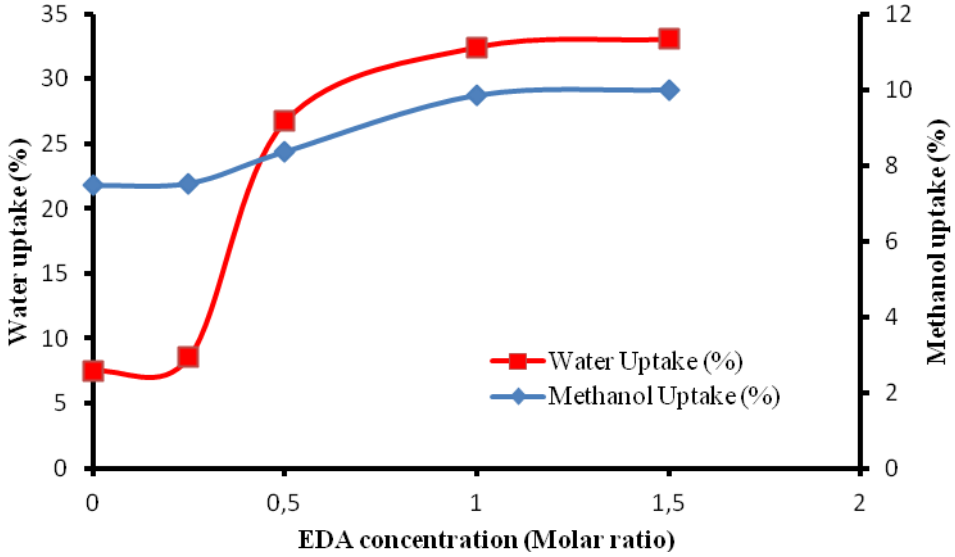

Figure 5a. Water and methanol uptakes of AMCA films at different EDA concentration at 45 °C for 8 h.

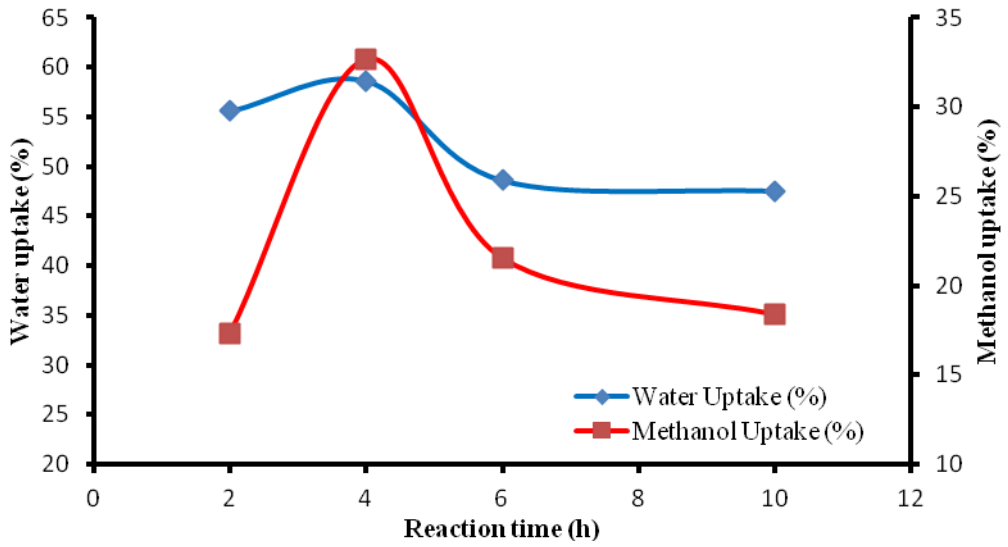

Figure 5b. Water and methanol uptakes of AMCA films using 1M EDA at a various time and 45 °C.

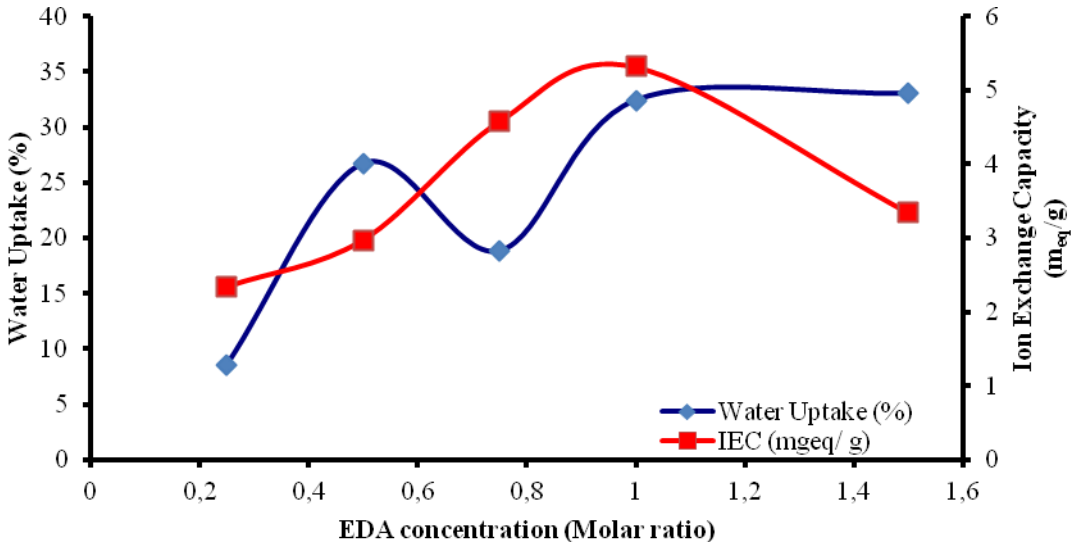

Figure 6. Water uptakes and IEC trend of AMCA films at different EDA concentration at 45 °C for 8 h.

3.2.2. Dimensional changes

Table 1a. Dimensional changes of AMCA membranes at different EDA concentration at 35 °C for 8 h

EDA concentration (M)	Dimension change in water (%)	Dimension change in methanol (%)
Original CA membrane	0.0	0.0
ACA membrane	2.5	5
AMCA membranes		
0.25	4	0.0
0.5	13.07	2
0.75	6	10.93
1	13.07	6.67
1.5	10.99	8.46

Table 1b. Dimensional changes of AMCA membranes using 1M EDA at different reaction time at 35 °C

Reaction time (h)	Dimensional change in water (%)	Dimensional change in methanol %
Original CA membrane	0.0	0.0
AMCA membranes		
2	13.07	0.0
4	13.07	10.93
8	13.07	6.67
10	13.07	18.41

The change in AMCA membranes dimensions after immersing in water or methanol for 24 h at different molar ratios of EDA and different amination time obtainable in Tables 1 (a and b). It was

concluded that the dimensions of all AMCA membranes clearly differed from that of the CA and ACA membranes. This result expected due to the introduction of hydrophilic amine groups [38].

3.2.3. Mechanical characteristics

Table 2 explains the positive force effect on the elongation of the modified membrane as a result of the amination process. The data revealed that the elongation of AMCA membrane is much advanced than that of the original and ACA films. The results proved that the AMCA membranes became more elastic upon the amination process in addition to the improvement of its mechanical properties.

Table 2. Mechanical characteristics of AMCA films at different EDA concentration at 45 °C for 8 h

EDA concentration (M)	Tensile strength (N)	Elongation (mm)
CA membrane	15.21	2.645
ACA membrane	45.45	7.75
AMCA membranes		
0.25	31.37	4.65
0.5	31.1	6.88
0.75	27.62	9.50
1	32.13	12.4

3.2.4. Optical properties (Color test)

Table 3a. Optical behavior of AMCA membranes at several EDA concentrations at 45 °C for 8 h

EDA concentration (M)	L*	a*	b*	ΔE*
CA membrane	88.04	+0.08	-8.083	49.67
ACA membrane	86.91	+0.07	-8.21	48.88
AMCA membranes				
0.25	89.93	+0.793	+0.953	46.27
0.5	86.76	+2.347	+4.770	41.59
0.75	83.42	+5.603	+16.023	34.75
1	80.23	+10.657	+23.803	31.48
1.5	62.57	+19.693	+47.803	31.84

Table 3b. Optical parameters of AMCA membranes using IM EDA at different reaction time and 45 °C

Reaction time (h)	L*	a*	b*	ΔE*
CA membrane	88.04	+0.08	-8.083	49.67
AMCA membranes				
2	75.78	+12.60	+30.9	28.7
4	76.50	+9.11	+22.46	20.93
6	71.30	+15.06	+23.83	28.55
8	80.23	+10.66	+23.80	31.48
10	66.17	+18.13	+39.06	27.41

Upon the amination process, the AMCA membranes have a slight brown color distinguish them from the colorless CA and ACA membranes, so the effective change in the optical parameters was expected upon the amination process as shown in Tables 3 (a and b).

3.2.5. Surface roughness test

The surface roughness measurements of the upper and lowered surface of AMCA membrane surface was illustrated in Table 4. By comparing the obtained data, it was observable that there was a noteworthy change in the membranes surface as a result of the amination process.

Table 4. Surface roughness parameters for AMCA films at various concentration of CA: ECH: EDA, 8 h, and at 45 °C

EDA concentration (M)	Ra (µm) For upper surface	Ra (µm) For lower surface
CA membrane	0.05	0.08
ACA membrane	0.066	0.064
AMCA membranes		
0.25	0.038	0.06
0.5	0.044	0.078
0.75	0.04	0.04
1	0.085	0.093
1:3:1.5	0.105	0.146

3.2.6. Thermal oxidation stability

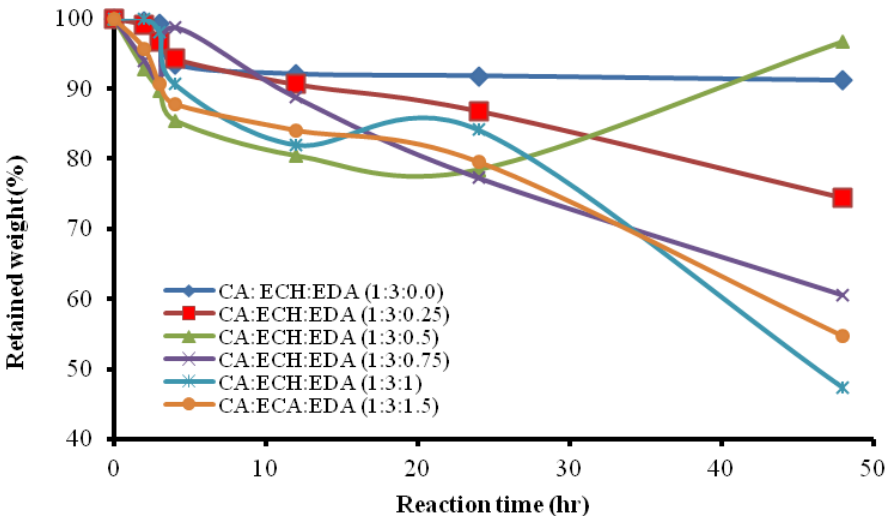

Figure 7. Thermal oxidation stability of AMCA membranes using different EDA concentration at 80 °C.

Figure 7 demonstrates that the AMCA membranes are highly thermally oxidatively stable under high temperature (up to 80 °C). Furthermore, the retained weight of AMCA membranes ranged from 50- 98% with increasing EDA concentration from 0.25 to 1.5 M comparing to 85% in case of ACA membrane. This outcome may be attributed to the hydrophilic character of AMCA which responsible for its weight loss [39].

3.2.7. FTIR analysis

Figure 8 demonstrates the FTIR spectra for original, ACA and AMCA membranes, through the presence of the typical absorption band of OH^- at 3498.99, 3489.34 and 3493.61 cm^{-1} for CA, ACA, and AMCA films. Also, –C=O absorption band appeared at 1732-1764 cm^{-1}, and the characteristic band for the epoxy ring at 1213cm^{-1} [47]. Furthermore, the manifestation of the particular band for NH_2 groups at 3493-3591 cm^{-1} exhibits the epoxy ring opening through amination process [42].

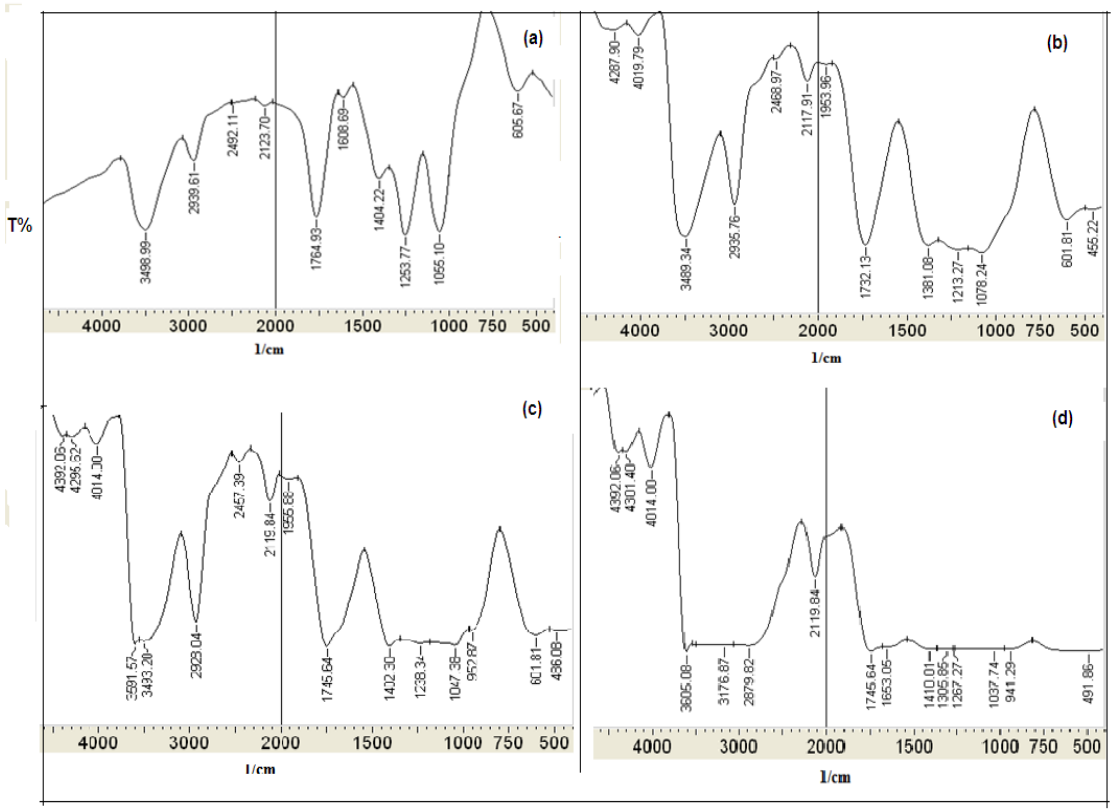

Figure 8. FTIR spectra of (a) original, (b) ACA, (c) AMCA [1 M EDA], and (d) AMCA [1.5M EDA] membranes.

3.2.8. Thermal gravimetrical analysis (TGA)

TGA results of the CA, ACA, and AMCA membranes are shown in Figure 9. The figure illustrates that the weight losses of the AMCA membrane completed near 600 °C with three separate

weight losses steps from 100–130, 300–350, and from 500-600 °C. Furthermore, it was apparent from Table 5 that at T_{50} = 320.38 °C the AMCA membrane mislaid about 50% of its original mass which proves that amination process enhanced the hydrophilicity of CA membrane to a great extent due to introducing the hydrophilic amine groups. In general, the degradation temperature of AMCA membrane (Td) is high enough for DMFC applications as it is about 320.38 °C.

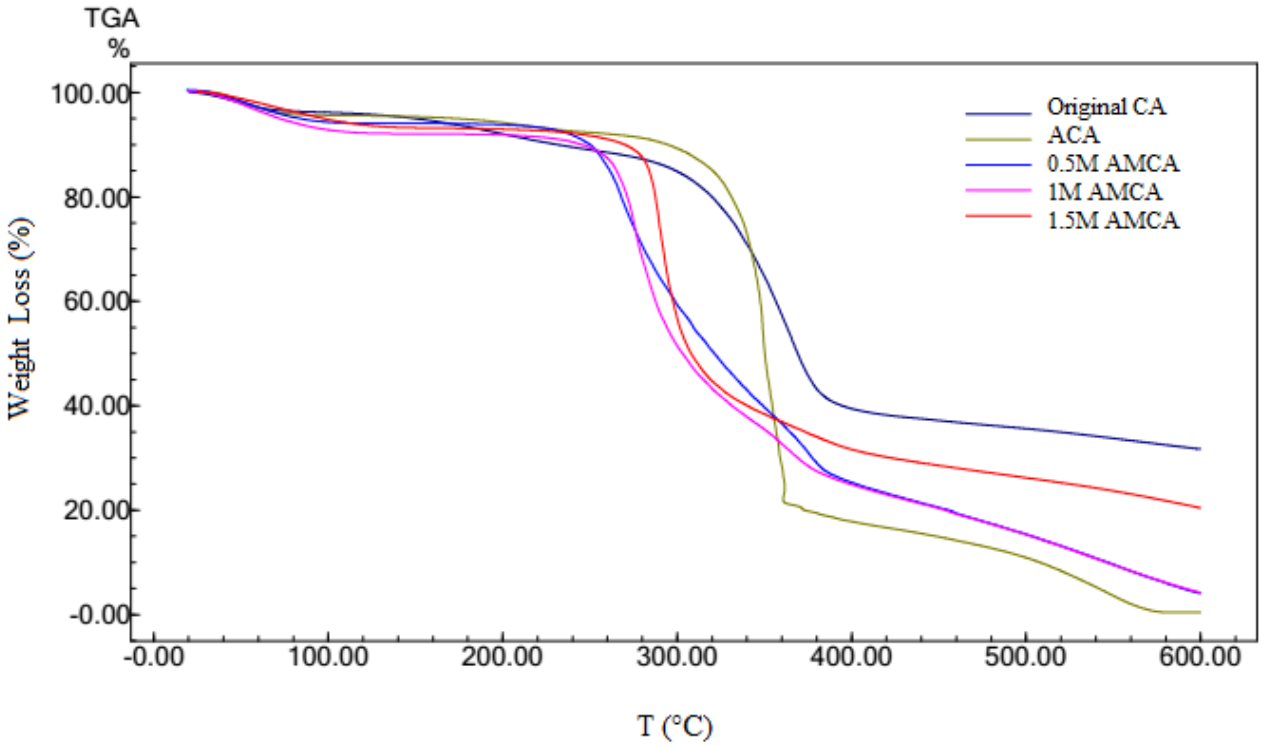

Figure 9. TGA thermograph of original, ACA, and AMCA films**.**

Table 5. TGA analysis for CA, ACA and AMCA membranes

EDA concentration (M)	T_{50} °C	Weight losses (%) at a temperature range (0-150 °C)
CA membrane	360.83	4.611
ACA membrane	350.23	4.75
AMCA membrane 0.5	302.82	8.127
1	307.91	6.863
1.5	320.47	6.497

3.2.9. Morphological characterization (SEM)

Figure 10 discuses the change in morphological structures in both surface and cross section of original, ACA and AMCA membranes. The figures revealed that the morphological structure of

AMCA membranes differed from that of both original CA and ACA membranes, which indicates that the structure has been as a consequence of the amination reaction [42].

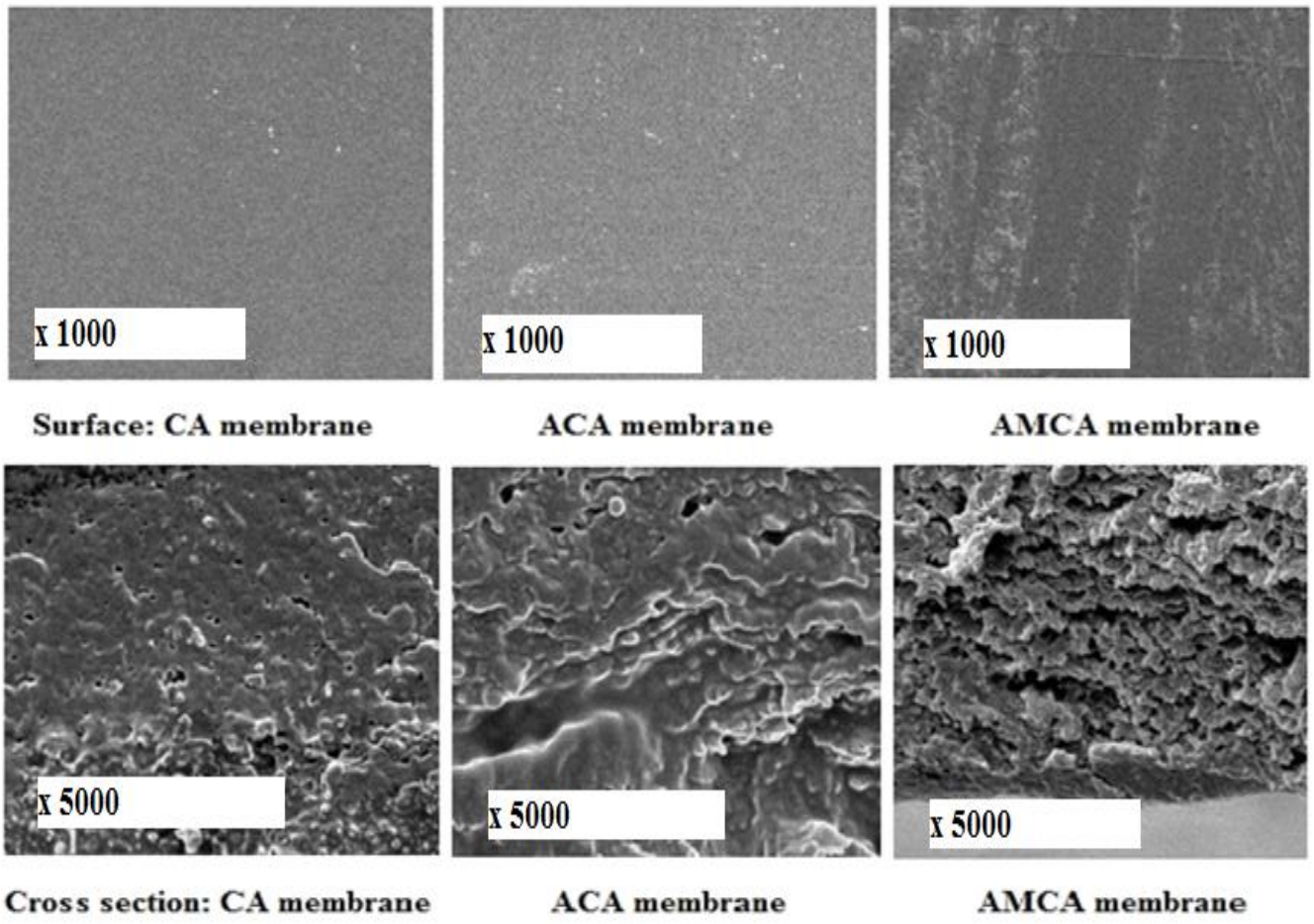

Figure 10. SEM of CA, ACA, and AMCA films (surface and cross section).

3.2.10. Methanol permeability measurements

The methanol crossover of AMCA membranes (1M) was evaluated through the incline of the plotted line between the permeation time and methanol concentration as represented in Figure 11. The results showed that the permeated methanol across the modified membrane (4.54*10-17 cm^2/S) is greatly lesser than that of Nafion®117 films [48] due to the presence of aminated groups which act as a blockade for methanol crossover across the membrane structure. Similar observations were also made by other authors [38, 39, 42].

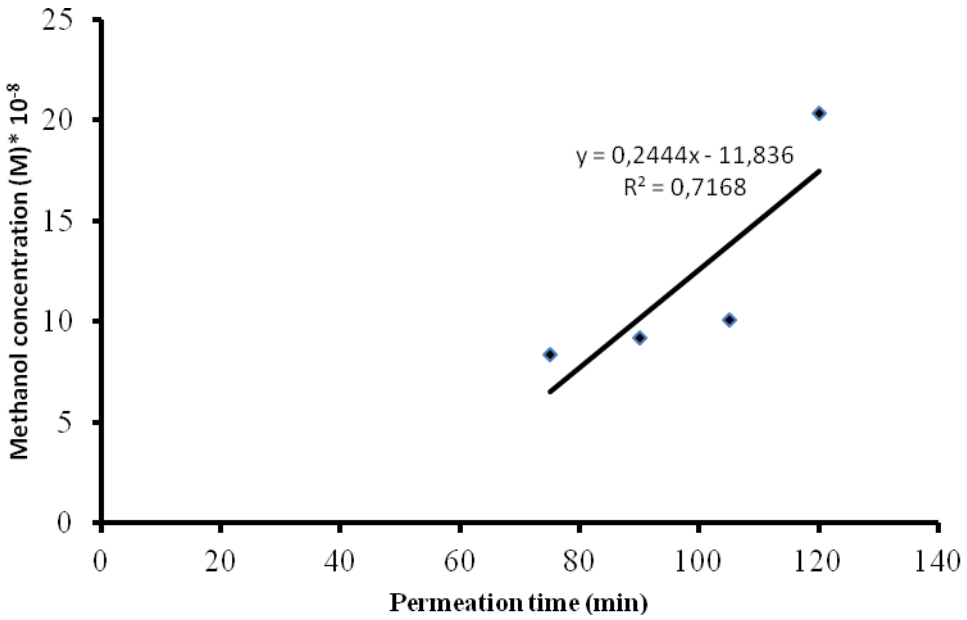

Figure 11. Methanol concentration as a function of time for the AMCA membrane.

3.2.11. Membrane performance (membrane efficiency)

The membranes in DMFCs required high IC and less methanol permeability, and as the IEC is acting as a meter for the PC, So, the ratio between the membrane IEC and its methanol permeability is used as one of the indicators of the membrane performance in DMFCs (performance factor) [49]. The data was represented graphically as a function of EDA concentrations in Figure 12.

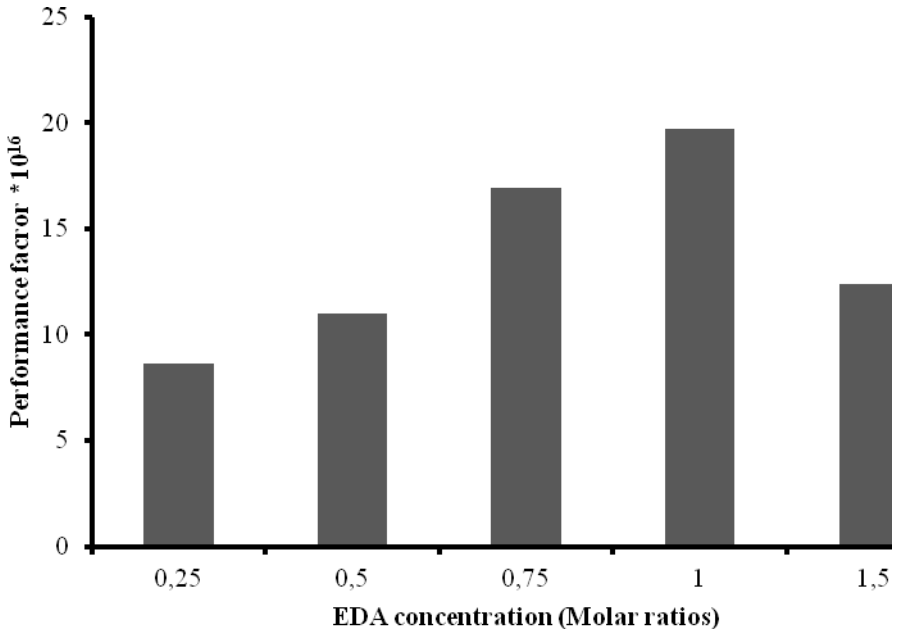

Figure 12. Performance factor as a function of EDA concentration for the AMCA membrane.

It was evident from the figure that the efficiency feature for all modified CA membranes is

advanced than that of commercial Nafion®117 membranes ($3.12*10^{-7}$) with maximum efficiency factor at 1 M EDA concentration. This result makes the AMCA membranes are expected candidate in applications of DMFC [39].

4. CONCLUSION

In this study, a successful synthesis of a novel PEM based on CA structure was performed through the reaction with EDA. The prepared AMCA membranes show lesser LU in water and methanol, excellent chemical and thermal stability, sufficient dimensional stability, and enhanced mechanical characteristics. Additionally, IEC of the prepared AMCA membranes ranged from 2.34-5.319 meq/g with the disparity in EDA concentration from 0.25 - 1M. What's more, the methanol crossover across the customized membranes (1M EDA) was $4.54*10^{-17}$ cm^2/S compared to $1.14*10^{-9}cm^2/S$ of Nafion®117 which confirmed that the AMCA have outstanding methanol barrier properties. More important, the efficiency factor (membrane performance) of AMCA films is much elevated than that of Nafion®117 membranes. Thus, the experimental results recommend that the synthesized AMCA offer excellent potential for use as PEM in DMFCs applications.

References

1. D. J. Jones, J. Rozière, *J Membrane Sci*., 185 (2001) 41–58.
2. C. M. Branco, S. Sharma, M. M. C. Forte, R. S. Wilckens, *J power sources*. 316 (2016) 139-159.
3. N. T. Q. Chi, D. X. Luu, D. Kim, *Solid State Ionics*. 187 (2011) 78-84.
4. S.P. Jiang, Z. Liu, Z.Q. Tian, *Adv. Mater*. 18 (2006) 1068–1072.
5. L. Vilčiauskas, M.E. Tuckerman, G. Bester, S. J. Paddison, K.D. Kreuer, *Nat. Chem.* 4 (2012) 461–466.
6. J. Choi, D. H. Kim, H. K. Kim, C. Shin, S. C. Kim, *J Membrane Sci*. 310, 384 (2008).
7. Y.E. Sung, *Electrochimica Acta*. 50 (2004) 583-588.
8. K.D. Kreuer, *J Membrane Sci*. 185 (2001) 29-39.
9. B. C. H. Steele, A. Heinzel, *Nature*. 414 (2001) 345-352.
10. M. A. Hickner, H. Ghassemi, Y. S. Kim, B. R. Einsla, J. E. McGrath, *Chem. Rev*.104 (2004) 4587–4612.
11. Y. Woo, S.Y. Oh, Y.S. Kang, B. Jung, *J Membrane Sci*. 220 (2003) 31–45.
12. N. Gourdoupi, A.K. Andreopoulou, V. Deimede, J.K. Kallitsis, *Chem. Mater*. 15 (2003) 5044–5050.
13. S. Tan, D. Belanger, *J. Phys. Chem*. B, 109(2005) 23480- 23490.
14. S.H. Min, D.J. Kim, *Solid State Ionics*. 180 (2010) 1690–1693.
15. C.H. Huang, H.M. Wu, C.C. Chen, C.W. Wang, P.L. Kuo, *J Membrane Sci.* 353 (2010) 1–9.
16. A. Kuver, I. Vogel, W. Vielstich, *J Power Sources*. 52 (1994) 77–80.
17. L. Jorissen, V. Gogel, J. Kerres, J. Garche, *J Power Sources* 105 (2002) 267–273.
18. R. Devanathan, *Energy Environ Sci*. 1 (2008) 101-119.
19. S. J. Peighambardoust, S. Rowshanzamir, M. Amjadi, *Int J Hydrogen Energy*. 35 (2010) 9252-9260.
20. J.V. Gasa, R.A. Weiss, M.T. Shaw, *J Membrane Sci*. 320 (2008) 215–223.
21. T. P. Nonjola, M. K. Mathe, R. M. Modibedi, *Int J Hydrogen Energy*. 38 (2013) 5115-5121.
22. S. M. J. Zaidi, S. D. Mikhailenko, G. P. Robertson, M. D. Guiver, S. J. Kaliaguine, *J Membrane Sci*. 173 (2000) 17–34.

23. C. Genies, R. Mercier, B. Sillion, N. Cornet, G. Gebel, M. Pineri, *Polymer*. 42 (2001) 359–373.
24. B.Y. Wang, C. K. Tseng, C. M. Shih, Y. L. Pai, H. P. Kuo, S. J. Lue, *J Membrane Sci.* 464 (2014) 43-54.
25. F. Gong, N. Li, S. Zhang. *Polymer.* 50 (2009) 6001-6008.
26. N. Li, S. Li, S. Zhang, J. Wang. *J Power Sources*. 187 (2009) 67-73.
27. M. Han, G. Zhang, Z. Liu, S. Wang, M. Li, J. Zhu, *J Materia Chemistry*; 21(2011) 2187- 2193.
28. Q. Guo, P.N. Pintauro, H. Tang, S. O'Connor, *J Membrane Sci*. 154 (1999) 175–181.
29. Y. Gao, G. P. Robertson, M. D. Guiver, X. G. Jian, S. D. Mikhailenko, K. P. Wang, S. Kaliaguine, *J Membrane Sci*. 227 (2003) 39–50.
30. Y. M. Sun, T. C. Wu, H. C. Lee, G. B. Jung, M. D. Guiver, Y. Gao, Y. L. Liu, J. Y. Lai, *J Membrane Sci.* 265 (2005) 108- 114.
31. T. Xu, D. Wu, L. Wu, *Prog. Polym. Sci*. 33 (2008) 894- 915.
32. B. J. Liu, G. P. Robertson, M. D. Guiver, Y. M. Sun, Y. L. Liu, J.Y. Lai, S. Mikhailenko, S. Kaliaguine, *J Polym Sci. Part B: Polym. Phys*. 44 (2006) 2299.
33. K. B. Wiles, F. Wang, J. E. McGrath, *J Polym Sci. Part A: Polym. Chem*. 43 (2005) 2964.
34. P. Costamagna, C. Yang, A. B. Bocarsly, S. Srinivasan, *Electrochimica Acta*. 47 (2002) 1023–1033.
35. J. Wang, R. He, *Solid State Ionics*. 278 (2015) 49-57.
36. J. M. Yang, N. C. Wang, H. C. Chiu, *J Membrane Sci*. 457 (2014) 139–148.
37. N. Kakati, J. Maiti, G. Das, S. H. Lee, Y. S. Yoon, *Int J Hydrogen Energy*. 40 (2015) 7114–7123.
38. M. S. Mohy Eldin, M. H. Abd Elmageed, A. M. Omer, T. M. Tamer, M. E. Yossuf, R. E. Khalifa, *Int J Electrochem Sci*. 11 (2016) 3467 - 3491.
39. M. S. Mohy Eldin, M. H. Abd Elmageed, A. M. Omer, T. M. Tamer, M. E. Yossuf, R. E. Khalifa, *Int J Electrochem Sci. Accepted Manuscript*, 11 (2016).
40. M. Theodor, N. Raluco, I.P. Valentin, *bioresources*. 3 (2008) 1371-1376.
41. C. Yang, W. Chien, Y. J. Li, *Int J Hydrogen Energy*. 36 (2010) 3407- 3415.
42. M. S. Mohy Eldin, A. A. Elzatahry, K. M. El-Khatib, E. A. Hassan, M. M. El-Sabbah, M. A. Abu-Saied, *J Appl Polym Sci*, 119 (2011) 120–133.
43. M. M. Nasef , N. A. Zubir , A. F. Ismail , M. Khayet , K. Z. M. Dahlan , H. Saidi , R. Rohani , T. I. S. Ngaha, N.A. Sulaiman. *J Membrane Sci*. 268 (2006) 96–108.
44. V. Tricoli. *J Electrochem Soc*. 145 (1998) 3798-3801.
45. R. E. Khalifa, PhD thesis, Alexandria University, Egypt, (2016).
46. T.A. Zawodzinski, C. Derouin, S. Radzinski, R. J. Sherman , V. T. Smith, T. E. Springer, S. Gottesfeld, *J Electrochem Society*, 140 (1993)1041-1047.
47. M. H.Woo, O. Kwon, S. H. Choi, M. Z. Hong, H. W. Ha, K. Kim, *Electrochimica Acta*, 51 (2006) 6051–6059.
48. A. B. A. Amine, MSc thesis, Faculty of Science AL-Azhar University, Egypt, (2007).
49. J. C. W. Waker, *J Electrochem Society*. 151(2004)1797-1803.